Optics & Laser Technology 50 (2013) 78–86

Contents lists available at SciVerse ScienceDirect

Optics & Laser Technology

journal homepage: www.elsevier.com/locate/optlastec

Propagation properties of partially coherent higher-order cosh-Gaussian beam in non-Kolmogorov turbulence

Huafeng Xu [a,b], Zhifeng Cui [a], Jun Qu [a,*], Wei Huang [b,*]

[a] Department of Physics, Anhui Normal University, Wuhu 241000, China
[b] Laboratory of Atmospheric Physico-Chemistry, Anhui Institute of Optics & Fine Mechanics, Chinese Academy of Sciences, Hefei, Anhui 230031, China

ARTICLE INFO

Article history:
Received 17 November 2012
Received in revised form
7 January 2013
Accepted 24 January 2013
Available online 22 March 2013

Keywords:
Huygens–Fresnel principle
Partially coherent higher-order cosh-Gaussian beams
Non-Kolmogorov turbulence

ABSTRACT

Based on the extended Huygens–Fresnel principle and second-order moments of the Wigner distribution function (WDF), the analytical formulation for the average intensity, the root-mean-square (rms) beam width and M^2-factor of partially coherent higher-order cosh-Gaussian (ChG) beams propagating in non-Kolmogorov turbulence are derived. The influences of the beam parameters and the spectrum parameters associated with the non-Kolmogorov turbulence on the propagation properties of partially coherent higher-order ChG beams in non-Kolmogorov turbulence are numerically investigated. Numerical results reveal that partially coherent higher-order ChG beams with higher beam order, larger decentered parameter and smaller coherence length are less affected by the turbulence. Furthermore, it is found that the beams will be more affected by the turbulence with smaller inner scale, larger outer scale or larger structure constant. In addition, numerical results reveal that the propagation properties of beams in non-Kolmogorov turbulence are largely dependent on the generalized exponent α, the structure constant, the inner and outer scale, which is much different from that in the case of Kolmogorov turbulence. This research may be useful for the practical applications of partially coherent higher-order ChG beams in connection with optical communications and the remote sensing.

1. Introduction

For a long time, the studies on beams propagation are mainly based on Kolmogorov′s power spectrum of refractive index fluctuations. However, in last several decades, both experimental results [1] and theoretical investigations [2] have pointed out that turbulence in portions of troposphere and stratosphere deviates from predictions of the Kolmogorov model. Since the vertical component is suppressed when the atmosphere is extremely stable, the turbulence is no longer homogeneous in three dimensions. Therefore, it is very important and necessary to find new models for the solution of this anomalous behavior. Fortunately, Toselli et al. proposed a new theoretical spectrum model, known as non-Kolmogorov power spectrum [3], by using a power-law parameter "α" instead of a constant standard exponent value 11/3, and a generalized amplitude factor instead of constant value 0.033. It is meaningful to analyze the impact of non-Kolmogorov nature of the spectrum on beams propagation when one is dealing with optical communication over slant atmospheric paths or over the horizontal paths in upper layers of the atmosphere. So far, based on this non-Kolmogorov power spectrum, a considerable number of interesting work has been presented, such as second-order statistics of stochastic electromagnetic beams [4], beam propagation factor of partially coherent Laguerre–Gaussian and Hermite–Gassian beams [5,6], propagation of elegant Laguerre–Gaussian beam and cosh-Gaussian beam [7–9], average spreading of a Gaussian beam array [10,11], angle of arrival fluctuations for free space laser beam propagation [12], scintillation behavior of cosh Gaussian beams [13] and so on.

In recent years, as a special case of Hermite–sinusoidal-Gaussian (HSG) beam, the ChG beam and its propagation characteristics have attracted extensive attention due to its practical applications [8,9,13–19]. It is well known that a ChG beam can be regarded as the superposition of four decentered Gaussian beams with the same waist width. A group of virtual sources that generate a ChG beam has been proposed [14]. Various intensity profiles can be derived by a suitable choice of beam parameters [8,9] and used in the space diversity applications in free-space optics (FSO) systems. Considerable theoretical investigations of ChG beams have been proposed to study the propagation properties in the present of turbulence atmosphere. For instance, the scintillation [13,16], the polarization [17], and the reciprocity between the cos- and cosh-Gaussian beams [18] were investigated by Eyyuboğlu. Chu and

* Corresponding authors. Tel.: +86 5533883561.
E-mail addresses: qujun70@mail.ahnu.edu.cn (J. Qu), huangwei@aiofm.ac.cn (W. Huang).

0030-3992/$ - see front matter Crown Copyright © 2013 Published by Elsevier Ltd. All rights reserved.
http://dx.doi.org/10.1016/j.optlastec.2013.01.025

Zhou studied the propagation factor [19] and the kurtosis parameter [20] of ChG beams in a turbulence atmosphere. The properties of cosh-Gaussian and partially coherent cos-Gaussian beams through a paraxial *ABCD* optical system in turbulent atmosphere have been demonstrated [15,21]. Angular spread of partially coherent Hermite–ChG beams through atmospheric turbulence has been examined [22]. The behaviour of ChG beams and elliptical ChG beams diffracted by a circular aperture in turbulent atmosphere were evaluated [23,24]. More recently, the higher-order ChG beams, as the special cases of ChG beams, have also been extensively investigated [25,26].

Partial coherence, originating from random phase shift and tilt, is a key ingredient of a laser beam. Thus it is of practical significance to incorporate partial coherence into beams and discuss the influence of the spatial coherent length on the propagation properties in turbulence atmosphere. Recently, more and more attention is being paid to the investigation of partially coherent beams in turbulence atmosphere [27–32], which have shown that partially coherent beams are less affected by turbulence than fully coherent beams. But to the best of our knowledge, the propagation of a partially coherent higher-order ChG beam in non-Kolmogorov turbulence has not been reported. In the present paper, our main motivations are to understand whether the use of partially coherent higher-order ChG beams as the special cases of ChG beams will improve system performance in turbulent atmosphere, and to study the properties of partially coherent higher-order ChG beams in non-Kolmogorov turbulence.

2. Theory

2.1. Average intensity and the rms beam width of a partially coherent higher-order ChG beam in turbulent atmosphere

In the Cartesian coordinate system, taking the z-axis as the propagation axis, the electric field distribution of higher-order ChG beam in the source plane ($z=0$) can be written as [25,26]

$$E_n(x_0,y_0,0)=\cosh^n(\Omega_0 x_0)\cosh^n(\Omega_0 y_0)\exp\left(-\frac{x_0^2+y_0^2}{w_0^2}\right),\quad n=1,2,3,\ldots \tag{1}$$

where n is the beam order, w_0 is the initial waist width of the Gaussian amplitude distribution, and Ω_0 which has the unit of m^{-1}, is the parameter associated with the cosh function. When $n=0$ and $n=1$, Eq. (1) reduces to be the well-known Gaussian beam and ChG beam, respectively. According to [26], the higher-order ChG beam can also be expressed as the form of superposition of $n+1$ decentered Gaussian beam with the same waist width

$$E_n(x_0,y_0,0)=\sum_{h=0}^{n}\sum_{l=0}^{n}\frac{1}{2^{2n}}\binom{n}{h}\binom{n}{l}\exp\left(\frac{p_h^2+p_l^2}{w_0^2}\right)\exp\left[-\frac{(x_0-p_h)^2+(y_0-p_l)^2}{w_0^2}\right] \tag{2}$$

where $p_h=(h-n/2)\delta w_0$ and $p_l=(l-n/2)\delta w_0$ with $\delta=w_0\Omega_0$ being the decentered parameter.

The fully coherent beam can be extended to the partially coherent one by incorporating the spectral degree of coherence into the source beam [27–32], the cross-spectral density function of a partially coherent higher-order ChG beam is generally characterized as

$$\begin{aligned}W^{(0)}(\boldsymbol{\rho}_1',\boldsymbol{\rho}_2',0,\omega)&=\langle E_n(\boldsymbol{\rho}_1',0)E_n^*(\boldsymbol{\rho}_2',0)\rangle\\&=\sum_{h_1=0}^{n}\sum_{l_1=0}^{n}\sum_{h_1=0}^{n}\sum_{l_1=0}^{n}\frac{1}{2^{4n}}\binom{n}{h_1}\binom{n}{l_1}\binom{n}{h_2}\binom{n}{l_2}\\&\quad\exp\left[\frac{p_{h_1}^2+p_{l_1}^2}{w_0^2}\right]\exp\left[-\frac{(x_1'-p_{h_1})^2+(y_1'-p_{l_1})^2}{w_0^2}\right]\\&\quad\times\exp\left(\frac{p_{h_2}^2+p_{l_2}^2}{w_0^2}\right)\exp\left[-\frac{(x_2'-p_{h_2})^2+(y_2'-p_{l_2})^2}{w_0^2}\right]\\&\quad\exp\left[-\frac{(x_1'-x_2')^2+(y_1'-y_2')^2}{2\sigma_0^2}\right]\end{aligned} \tag{3}$$

where $\boldsymbol{\rho}'=(x',y')$ is the transverse coordinates in the source plane, $\langle\bullet\rangle$ denotes averaging over the field ensemble, σ_0 is the spatial correlation length of partially coherent higher-order ChG beams at the source plane. Eq. (3) reduces to the cross-spectral density of a coherent higher-order ChG beams when $\sigma_0\to\infty$.

By using the extended Huygens–Fresnel principle [9,27–32], the cross-spectral density of a partially coherent higher-order ChG beams propagating in turbulence atmosphere can be obtained by

$$\begin{aligned}W(\boldsymbol{\rho}_1,\boldsymbol{\rho}_2,z,\omega)&=\left(\frac{k}{2\pi z}\right)^2\int\int\int\int d^2\boldsymbol{\rho}_1' d^2\boldsymbol{\rho}_2' W^{(0)}(\boldsymbol{\rho}_1',\boldsymbol{\rho}_2',0,\omega)\\&\quad\times\exp\left\{-\frac{ik}{2z}\left[(\boldsymbol{\rho}_1-\boldsymbol{\rho}_1')^2-(\boldsymbol{\rho}_2-\boldsymbol{\rho}_2')^2\right]-H(\boldsymbol{\rho}_1',\boldsymbol{\rho}_2',z)\right\}\end{aligned} \tag{4}$$

where $k=2\pi/\lambda$ and λ denote the wave number and the wavelength, respectively.

$$\begin{aligned}H(\boldsymbol{\rho}_1',\boldsymbol{\rho}_2',z)&=\left\langle\exp[\psi(\boldsymbol{\rho}_1,\boldsymbol{\rho}_1',z)+\psi^*(\boldsymbol{\rho}_2,\boldsymbol{\rho}_2',z)]\right\rangle_m\\&=\exp\{-T(\alpha,z)[(\boldsymbol{\rho}_1-\boldsymbol{\rho}_2)^2+(\boldsymbol{\rho}_1-\boldsymbol{\rho}_2)(\boldsymbol{\rho}_1'-\boldsymbol{\rho}_2')+(\boldsymbol{\rho}_1'-\boldsymbol{\rho}_2')^2]\}\end{aligned} \tag{5}$$

$\psi(\boldsymbol{\rho},\boldsymbol{\rho}')$ represents the random part of the complex phase of a spherical wave that propagates from the source point $(\boldsymbol{\rho}_1',0)$ to the receiver point$(\boldsymbol{\rho}_1,0)$, and the term of $\langle\bullet\rangle_m$ denotes the average over the ensemble of the turbulence medium statistics, and the asterisk means the complex conjugate. Here, the term $T(\alpha,z)$ is set as a quantity to describe the strength of turbulence perturbation, which will be discussed in detail in Section 2.3.

On substituting from Eqs. (3) and (5) into Eq. (4), we obtain the average intensity of partially coherent ChG beams propagating in non-Kolmogorov turbulence

$$\begin{aligned}\langle I(\boldsymbol{\rho},z)\rangle&=\frac{k^2}{4\alpha_1\alpha_2 z^2}\sum_{h_1=0}^{n}\sum_{l_1=0}^{n}\sum_{h_2=0}^{n}\sum_{l_2=0}^{n}\frac{1}{2^{4n}}\binom{n}{h_1}\binom{n}{l_1}\binom{n}{h_2}\binom{n}{l_2}\\&\quad\exp\left(\frac{\beta_{1x}^2+\beta_{1y}^2}{\alpha_1}+\frac{\beta_{2x}^2+\beta_{2y}^2}{\alpha_2}\right)\end{aligned} \tag{6}$$

where

$$\begin{aligned}&E=\frac{1}{2\sigma_0^2}+T(\alpha,z),\quad \alpha_1=\frac{1}{w_0^2}+\frac{1}{2\sigma_0^2}+\frac{ik}{2z}+T(\alpha,z),\quad \alpha_2=\alpha_1^*-\frac{E^2}{\alpha_1}\\&\beta_{1x}=\frac{p_{h_1}}{w_0^2}+\frac{ik}{2z}x,\quad \beta_{2x}=\frac{p_{h_2}}{w_0^2}-\frac{ik}{2z}x+\frac{E}{\alpha_1}\beta_{1x},\quad \beta_{1y}=\frac{p_{l_1}}{w_0^2}+\frac{ik}{2z}y,\\&\beta_{2y}=\frac{p_{l_2}}{w_0^2}-\frac{ik}{2z}y+\frac{E}{\alpha_1}\beta_{1y}\end{aligned} \tag{7}$$

We have further studied the rms beam width to examine the spreading properties of partially coherent higher-order ChG beams in non-Kolmogorov turbulence, and the rms beam width is defined as [10,11,31]

$$W_\rho(z)=\sqrt{4\int_{-\infty}^{\infty}\int_{-\infty}^{\infty}\rho^2\langle I(x,y,z)\rangle dxdy\Big/\int_{-\infty}^{\infty}\int_{-\infty}^{\infty}\langle I(x,y,z)\rangle dxdy},\quad(\rho=x,y) \tag{8}$$

On substituting from Eq. (6) into Eq. (8), the analytical formulae for the rms beam width of partially coherent higher-order ChG beams in non-Kolmogorov turbulence is derived. Owing to the symmetry of the rms beam widths in x-direction

and in y-direction, we obtain

$$W_x(z)=W_y(z)=\sqrt{\frac{4G_1}{G_2}} \tag{9}$$

with

$$G_1=\sum_{h_1=0}^{n}\sum_{l_1=0}^{n}\sum_{h_2=0}^{n}\sum_{l_2=0}^{n}\binom{n}{h_1}\binom{n}{l_1}\binom{n}{h_2}\binom{n}{l_2}\left(\frac{1}{\alpha_3}+2\frac{\xi_1^2}{\alpha_3^2}\right)\exp\left(\frac{p_{h_1}^2+p_{l_1}^2}{\alpha_1 w_0^4}+\frac{\tau_1^2+\tau_2^2}{\alpha_2}+\frac{\xi_1^2+\xi_2^2}{\alpha_3}\right) \tag{10a}$$

$$G_2=\sum_{h_1=0}^{n}\sum_{l_1=0}^{n}\sum_{h_2=0}^{n}\sum_{l_2=0}^{n}\binom{n}{h_1}\binom{n}{l_1}\binom{n}{h_2}\binom{n}{l_2}\exp\left(\frac{p_{h_1}^2+p_{l_1}^2}{\alpha_1 w_0^4}+\frac{\tau_1^2+\tau_2^2}{\alpha_2}+\frac{\xi_1^2+\xi_2^2}{\alpha_3}\right) \tag{10b}$$

$$\alpha_3=\frac{k^2}{4z^2}\left[\frac{1}{\alpha_1}+\frac{1}{\alpha_2}\left(\frac{E}{\alpha_1}-1\right)^2\right],\quad \tau_1=\frac{1}{w_0^2}\left(\frac{E}{\alpha_1}p_{h_1}+p_{h_2}\right),\quad \tau_2=\frac{1}{w_0^2}\left(\frac{E}{\alpha_1}p_{l_1}+p_{l_2}\right) \tag{10c}$$

$$\xi_1=\frac{ik}{2z}\left[\frac{p_{h_1}}{\alpha_1 w_0^2}+\frac{\tau_1}{\alpha_2}\left(\frac{E}{\alpha_1}-1\right)\right],\quad \xi_2=\frac{ik}{2z}\left[\frac{p_{l_1}}{\alpha_1 w_0^2}+\frac{\tau_2}{\alpha_2}\left(\frac{E}{\alpha_1}-1\right)\right] \tag{10d}$$

Eqs. (6)–(10) can be used conveniently to study the average intensity and the rms beam width of partially coherent higher-order ChG beams in non-Kolmogorov turbulence.

2.2. WDF and M^2-factor of partially coherent higher-order ChG beams in turbulent atmosphere

By using the paraxial form of the extended Huygens–Fresnel principle, the cross-spectral density of partially coherent higher-order ChG beams propagating in turbulence atmosphere can be obtained by [5,6,27–29]

$$W(\boldsymbol{\rho},\boldsymbol{\rho}_d,z)=\left(\frac{k}{2\pi z}\right)^2\iint W(\boldsymbol{\rho}',\boldsymbol{\rho}_d',0)\exp\left\{\frac{ik}{z}\left[(\boldsymbol{\rho}-\boldsymbol{\rho}')\cdot(\boldsymbol{\rho}_d-\boldsymbol{\rho}_d')\right]-H(\boldsymbol{\rho}_d,\boldsymbol{\rho}_d',z)\right\}d^2\boldsymbol{\rho}'d^2\boldsymbol{\rho}_d' \tag{11}$$

To evaluate the above equation, it is convenient to introduce new variables of integration

$$\boldsymbol{\rho}'=\frac{\boldsymbol{\rho}_1'+\boldsymbol{\rho}_2'}{2},\quad \boldsymbol{\rho}_d'=\boldsymbol{\rho}_1'-\boldsymbol{\rho}_2',\quad \boldsymbol{\rho}=\frac{\boldsymbol{\rho}_1+\boldsymbol{\rho}_2}{2},\quad \boldsymbol{\rho}_d=\boldsymbol{\rho}_1-\boldsymbol{\rho}_2 \tag{12}$$

and the cross-spectral density in the source plane can be expressed as

$$W(\boldsymbol{\rho}',\boldsymbol{\rho}_d',0)=\Gamma(\boldsymbol{\rho}_1',\boldsymbol{\rho}_2',0)=\Gamma\left(\boldsymbol{\rho}'+\frac{\boldsymbol{\rho}_d'}{2},\boldsymbol{\rho}'-\frac{\boldsymbol{\rho}_d'}{2},0\right) \tag{13}$$

Eq. (11) can be expressed in the following alternative form [5,6,27–29]

$$W(\boldsymbol{\rho},\boldsymbol{\rho}_d,z)=\left(\frac{1}{2\pi}\right)^2\iiint W\left(\boldsymbol{\rho}'',\boldsymbol{\rho}_d+\frac{z}{k}\boldsymbol{\kappa}_d,0\right)\times\exp\left[-i\boldsymbol{\rho}\cdot\boldsymbol{\kappa}_d+i\boldsymbol{\rho}''\cdot\boldsymbol{\kappa}_d-H\left(\boldsymbol{\rho}_d,\boldsymbol{\rho}_d+\frac{z}{k}\boldsymbol{\kappa}_d,z\right)\right]d^2\boldsymbol{\rho}''d^2\boldsymbol{\kappa}_d \tag{14}$$

In Eq. (14), the term $\exp\left[-H\left(\boldsymbol{\rho}_d,\boldsymbol{\rho}_d+\frac{z}{k}\boldsymbol{\kappa}_d,z\right)\right]$ represents the effect of the turbulence, and H can be written as

$$H(\boldsymbol{\rho}_d,\boldsymbol{\rho}_d',z)=\left(\frac{z^2}{k^2}\boldsymbol{\kappa}_d^2+3\frac{z}{k}\boldsymbol{\kappa}_d\boldsymbol{\rho}_d+3\boldsymbol{\rho}_d^2\right)T(\alpha,z) \tag{15}$$

where $\kappa_d=|\boldsymbol{\kappa}_d|=(\kappa_{dx}^2+\kappa_{dy}^2)^{1/2}$, and $\rho_d=|\boldsymbol{\rho}_d|=(\rho_{dx}^2+\rho_{dy}^2)^{1/2}$, and

$$\begin{aligned}W\left(\boldsymbol{\rho}'',\boldsymbol{\rho}_d+\frac{z}{k}\boldsymbol{\kappa}_d,0\right)&=W\left(x'',x_d+\frac{z}{k}\kappa_{dx},y'',y_d+\frac{z}{k}\kappa_{dy},0\right)\\&=\sum_{h_1=0}^{n}\sum_{l_1=0}^{n}\sum_{h_1=0}^{n}\sum_{l_1=0}^{n}\frac{1}{2^{4n}}\binom{n}{h_1}\binom{n}{l_1}\binom{n}{h_2}\binom{n}{l_2}\\&\times\exp\left[-\frac{2}{w_0^2}x''^2-\frac{1}{\varepsilon^2}\left(x_d+\frac{z}{k}\kappa_{dx}\right)^2+2A_hx''+B_h\left(x_d+\frac{z}{k}\kappa_{dx}\right)\right]\\&\times\exp\left[-\frac{2}{w_0^2}y''^2-\frac{1}{\varepsilon^2}\left(y_d+\frac{z}{k}\kappa_{dy}\right)^2+2A_ly''+B_l\left(y_d+\frac{z}{k}\kappa_{dy}\right)\right]\end{aligned} \tag{16}$$

with $1/\varepsilon^2=(1/2w_0^2)+(1/2\sigma_0^2)$, $A_h=(p_{h1}+p_{h2})/w_0^2$, $B_h=(p_{h1}-p_{h2})/w_0^2$, $A_l=(p_{l1}+p_{l2})/w_0^2$, and $B_l=(p_{l1}-p_{l2})/w_0^2$

It is well known that the WDF can characterize partially coherent beams in space and in spatial frequency domain simultaneously and can be expressed in terms of the cross-spectral density [5,6,27–29]

$$h(\boldsymbol{\rho},\boldsymbol{\theta},z)=\left(\frac{k}{2\pi}\right)^2\int_{-\infty}^{\infty}W(\boldsymbol{\rho},\boldsymbol{\rho}_d,z)\exp(-ik\boldsymbol{\theta}\cdot\boldsymbol{\rho}_d)d^2\boldsymbol{\rho}_d \tag{17}$$

where vector $\boldsymbol{\theta}=(\theta_x,\theta_y)$ denotes an angle of propagation, $k\theta_x$ and $k\theta_y$ is the wave vector component along the x-axis and y-axis, respectively.

Based on the second-order moments of WDF, the M^2-factor of beams can be defined as [27–29]

$$\begin{aligned}M^2(z)&=k\left(\langle\boldsymbol{\rho}^2\rangle\langle\boldsymbol{\theta}^2\rangle-\langle\boldsymbol{\rho}\cdot\boldsymbol{\theta}\rangle^2\right)^{1/2}\\&=k\left[\left(\langle x^2\rangle+\langle y^2\rangle\right)\left(\langle\theta_x^2\rangle+\langle\theta_y^2\rangle\right)-\left(\langle x\theta_x\rangle+\langle y\theta_y\rangle\right)^2\right]^{1/2}\end{aligned} \tag{18}$$

According to definition, moments of the order $n_1+n_2+m_1+m_2$ of WDF, it can be expressed as

$$\left\langle x^{n_1}y^{n_2}\theta_x^{m_1}\theta_y^{m_2}\right\rangle=\frac{1}{P}\iint x^{n_1}y^{n_2}\theta_x^{m_1}\theta_y^{m_2}h(\boldsymbol{\rho},\boldsymbol{\theta},z)d^2\boldsymbol{\rho}d^2\boldsymbol{\theta} \tag{19}$$

where

$$\begin{aligned}P&=\iint h(\boldsymbol{\rho},\boldsymbol{\theta},z)d^2\boldsymbol{\rho}d^2\boldsymbol{\theta}\\&=\frac{\pi w_0^2}{2}\frac{1}{2^{4n}}\sum_{h_1=0}^{n}\sum_{l_1=0}^{n}\sum_{h_2=0}^{n}\sum_{l_2=0}^{n}\binom{n}{h_1}\binom{n}{l_1}\binom{n}{h_2}\binom{n}{l_2}\\&\times\exp\left[\frac{w_0^2}{2}(A_h^2+A_l^2)\right]\end{aligned} \tag{20}$$

Substituting Eqs. (14)–(17) into Eq. (19), after some tedious integration, we obtain

$$\begin{aligned}\langle\boldsymbol{\rho}^2\rangle&=\langle x^2\rangle+\langle y^2\rangle\\&=\frac{1}{P}\frac{\pi w_0^2}{2}\frac{1}{2^{4n}}\sum_{h_1=0}^{n}\sum_{l_1=0}^{n}\sum_{h_2=0}^{n}\sum_{l_2=0}^{n}\binom{n}{h_1}\binom{n}{l_1}\binom{n}{h_2}\binom{n}{l_2}\\&\exp\left[\frac{w_0^2}{2}(A_h^2+A_l^2)\right]\\&\times\left\{\left(\frac{4}{\varepsilon^2}\frac{z^2}{k^2}+\frac{w_0^2}{2}+\frac{4z^2}{k^2}T(\alpha,z)\right)-\frac{z^2}{k^2}(B_h^2+B_l^2)+\frac{w_0^4}{4}(A_h^2+A_l^2)\right\}\end{aligned} \tag{21}$$

$$\begin{aligned}\left\langle\boldsymbol{\theta}^2\right\rangle&=\left\langle\theta_x^2\right\rangle+\left\langle\theta_y^2\right\rangle\\&=\frac{1}{P}\frac{\pi w_0^2}{2}\frac{1}{2^{4n}}\sum_{h_1=0}^{n}\sum_{l_1=0}^{n}\sum_{h_2=0}^{n}\sum_{l_2=0}^{n}\binom{n}{h_1}\binom{n}{l_1}\binom{n}{h_2}\binom{n}{l_2}\\&\times\exp\left[\frac{w_0^2}{2}(A_h^2+A_l^2)\right]\left[\frac{4}{k^2}\left(\frac{1}{\varepsilon^2}+3T(\alpha,z)\right)-\frac{1}{k^2}(B_h^2+B_l^2)\right]\end{aligned} \tag{22}$$

$$\langle \boldsymbol{\rho}\cdot\boldsymbol{\theta}\rangle = \langle x\theta_x\rangle + \langle y\theta_y\rangle = \frac{1}{P}\frac{\pi w_0^2}{2}\frac{1}{2^{4n}}\sum_{h_1=0}^{n}\sum_{l_1=0}^{n}\sum_{h_2=0}^{n}\sum_{l_2=0}^{n}\binom{n}{h_1}\binom{n}{l_1}\binom{n}{h_2}\binom{n}{l_2}\exp\left[\frac{w_0^2}{2}(A_h{}^2+A_l{}^2)\right] \times\left[\frac{z}{k^2}\left(\frac{4}{\varepsilon^2}+6T(\alpha,z)\right)-\frac{z}{k^2}(B_h{}^2+B_L{}^2)\right] \quad (23)$$

Substituting Eqs. (21)–(23) into Eq. (18), the expression of M^2-factor for partially coherent higher-order ChG beams in turbulent atmosphere can be expressed as

$$M^2(z) = k\left[\left(\langle x^2\rangle+\langle y^2\rangle\right)\left(\left\langle\theta_x^2\right\rangle+\left\langle\theta_y^2\right\rangle\right)-\left(\langle x\theta_x\rangle+\langle y\theta_y\rangle\right)^2\right]^{1/2} = k\left\{\left\{\frac{1}{P}\frac{\pi w_0^2}{2}\frac{1}{2^{4n}}\sum_{h_1=0}^{n}\sum_{l_1=0}^{n}\sum_{h_2=0}^{n}\sum_{l_2=0}^{n}\binom{n}{h_1}\binom{n}{l_1}\binom{n}{h_2}\binom{n}{l_2} \times\exp\left[\frac{w_0^2}{2}(A_h{}^2+A_l{}^2)\right]\times\left[\left(\frac{4}{\varepsilon^2}\frac{z^2}{k^2}+\frac{w_0^2}{2}+\frac{4z^2}{k^2}T(\alpha,z)\right) -\frac{z^2}{k^2}(B_h{}^2+B_l{}^2)+\frac{w_0^4}{4}(A_h{}^2+A_l{}^2)\right]\right\}\left\{\frac{1}{P}\frac{\pi w_0^2}{2}\frac{1}{2^{4n}}\sum_{h_1=0}^{n}\sum_{l_1=0}^{n}\sum_{h_2=0}^{n}\sum_{l_2=0}^{n} \times\binom{n}{h_1}\binom{n}{l_1}\binom{n}{h_2}\binom{n}{l_2}\exp\left[\frac{w_0^2}{2}(A_h{}^2+A_l{}^2)\right] \times\left[\frac{4}{k^2}\left(\frac{1}{\varepsilon^2}+3T(\alpha,z)\right)-\frac{1}{k^2}(B_h{}^2+B_l{}^2)\right]\right\} -\left\{\frac{1}{P}\frac{\pi w_0^2}{2}\frac{1}{2^{4n}}\sum_{h_1=0}^{n}\sum_{l_1=0}^{n}\sum_{h_2=0}^{n}\sum_{l_2=0}^{n}\binom{n}{h_1}\binom{n}{l_1}\binom{n}{h_2}\binom{n}{l_2} \times\exp\left[\frac{w_0^2}{2}(A_h{}^2+A_l{}^2)\right]\times\left[\frac{z}{k^2}\left(\frac{4}{\varepsilon^2}+6T(\alpha,z)\right)-\frac{z}{k^2}(B_h{}^2+B_L{}^2)\right]\right\}^2\right\}^{1/2} \quad (24)$$

2.3. Turbulence model

In the above sections, the term $T(\alpha,z)$ is set as a quantity to describe the strength of turbulence perturbation, and can be expressed as [3–13]

$$T(\alpha,z) = \frac{1}{3}\pi^2k^2z\int_{-\infty}^{\infty}\kappa^3\Phi_n(\kappa,\alpha)d\kappa \quad (25)$$

here κ is the magnitude of two-dimensional spatial frequency and $\Phi_n(\kappa,\alpha)$ denotes the spatial power spectrum of the refractive index fluctuations of the atmosphere turbulence. Including both the inner- and outer-scale effects, the non-Kolmogorov spectrum is defined as [3–13]

$$\Phi_n(\kappa,\alpha) = A(\alpha)\tilde{C}_n^2\frac{\exp[-(\kappa^2/\kappa_m^2)]}{(\kappa^2+\kappa_0^2)^{\alpha}},\quad 0\le\kappa<\infty,\quad 3<\alpha<4 \quad (26)$$

where $\kappa_0 = 2\pi/L_0$ with L_0 being the outer scale parameter and $\kappa_m = c(\alpha)/l_0$ with l_0 being the inner scale parameter, $c(\alpha) = [\Gamma(5-\alpha/2)\cdot A(\alpha)\cdot 2\pi/3]^{[1/(\alpha-5)]}$, the parameter α is the power-law exponent or the spectral index, $A(\alpha) = \Gamma(\alpha-1)\cos(\alpha\pi/2)/4\pi^2$ with $\Gamma(\bullet)$ being the gamma function, the term $\tilde{C}_n^2$ is the generalized structure parameter with unit of $m^{3-\alpha}$. When the power law approaches the limiting value $\alpha=3$, the function $A(\alpha)$ approaches zero and consequently the refractive-index power spectral density vanishes.

For non-Kolmogorov model, the integration over the spatial power spectrum in Eq. (25), one obtains

$$T(\alpha,z) = \frac{1}{3}\pi^2k^2z\int_0^{\infty}\kappa^3\Phi_n(\kappa,\alpha)d\kappa = \frac{\pi^2k^2zA(\alpha)\tilde{C}_n^2}{6}\frac{\kappa_m^{2-\alpha}\beta\exp(\kappa_0^2/\kappa_m^2)\Gamma(2-\alpha/2,\kappa_0^2/\kappa_m^2)-2\kappa_0^{4-\alpha}}{\alpha-2} \quad (27)$$

with $\beta = 2\kappa_0^2-2\kappa_m^2+\alpha\kappa_m^2$.

However, when $\alpha=11/3$, $A(\alpha)=0.033$, $L_0=\infty$, $l_0=0$ and $\tilde{C}_n^2 = C_n^2$, the spectrum expressed in Eq. (26) reduces to conventional Kolmogorov spectrum [3,10,11], and the spatial power spectrum of the refractive index fluctuations can be written as [31,32]

$$\Phi_n(\kappa) = 0.033C_n^2\kappa^{-11/3} \quad (28)$$

for Kolmogorov model [31,32]

$$T(11/3,z) = 1/\rho_0^2 \quad (29)$$

where $\rho_0 = (0.545C_n^2k^2z)^{-3/5}$ is the coherence length (induced by the atmospheric turbulence) of a spherical wave propagating in the turbulent medium with C_n^2 being the structure constant.

3. Numerical results and analysis

In this section, the evolution behavior of the normalized average intensity, the spreading of the rms beam width and the normalized M^2-factor of partially coherent higher-order ChG beams in non-Kolmogorov turbulence are discussed in detail. In

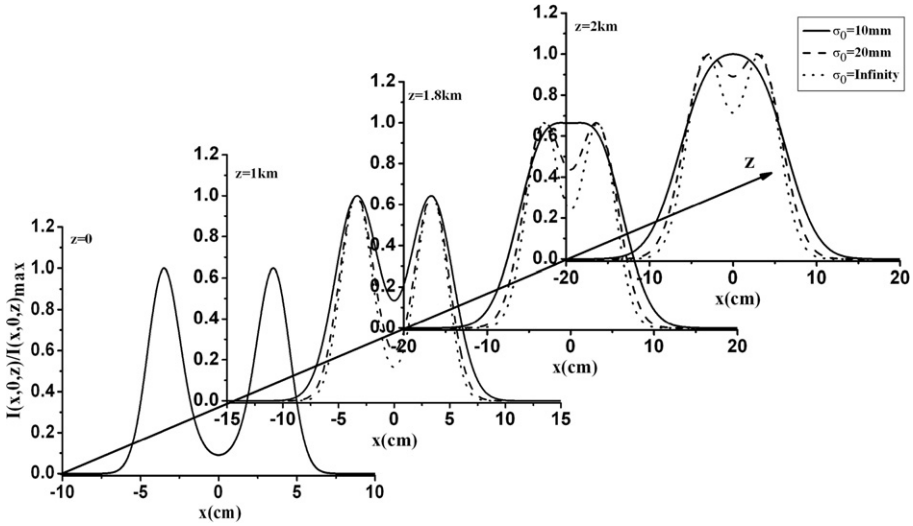

Fig. 1. The evolution of normalized average intensity distributions of coherent and partially coherent higher-order ChG beams propagating through non-Kolmogorov turbulence.

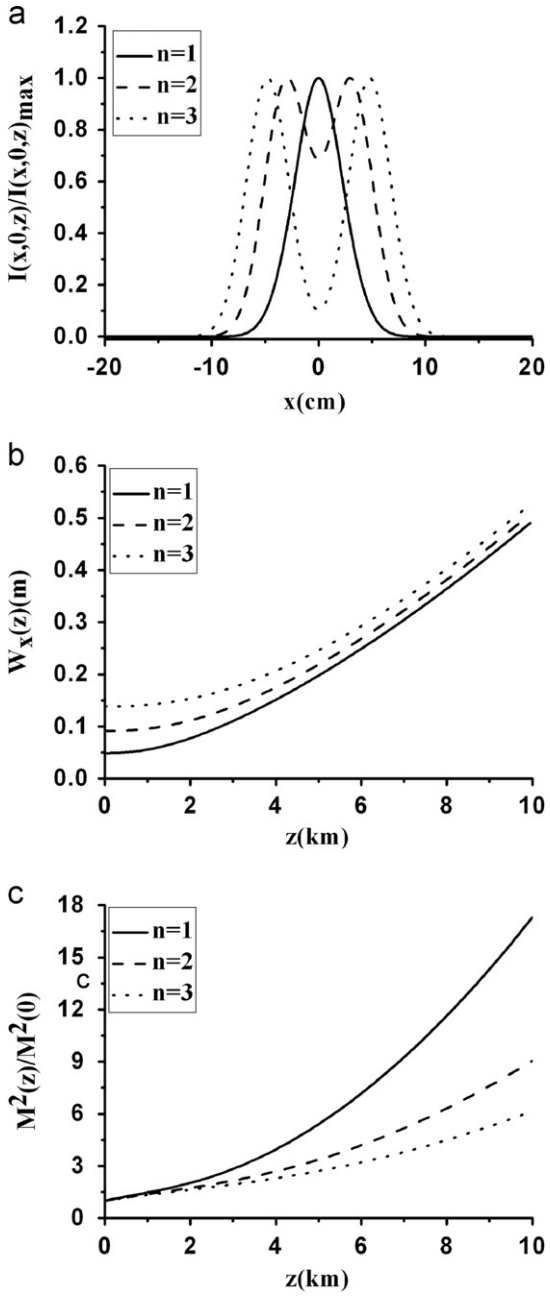

Fig. 2. Normalized average intensity distribution at $z=1.5$ km, the rms beam width and the normalized M^2-factor of partially coherent higher-order ChG beams for different values of beam order on propagation in non-Kolmogorov turbulence. The calculation parameters are $n=3$, $w_0=0.02$ m $\Omega_0=80$ m^{-1}, and $\sigma_0=0.02$ m,

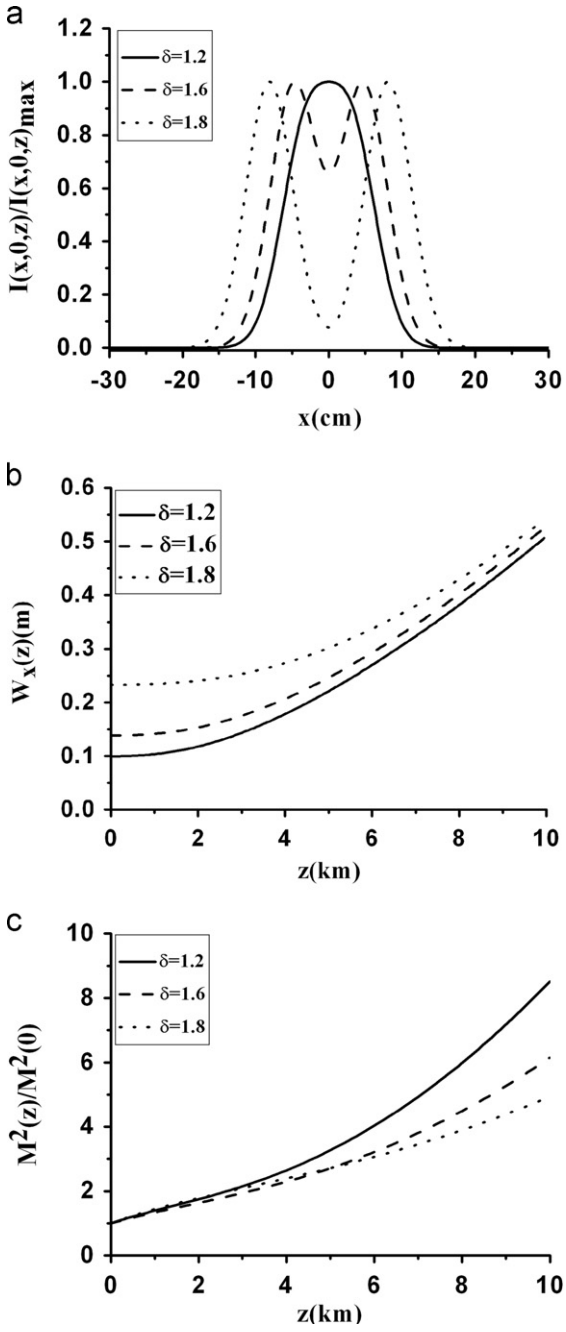

Fig. 3. Normalized average intensity distribution at $z=2$ km, the rms beam width and the normalized M^2-factor of partially coherent higher-order ChG beams for different values of the decentered parameter on propagation in non-Kolmogorov turbulence. The calculation parameters are $n=3$, and $\sigma_0=0.02$ m. The other calculation parameters are same as Fig. 1.

the source plane, the intensity profile of a partially coherent higher-order ChG beam can be obtained as a Gaussian-like beam, a flat-topped beam and a dark-hollow beam by a suitable choice of beam parameters; however, it is independent of the initial coherence. Without loss of generality, we take the dark-hollow beam as an example. The evolution behaviors of normalized average intensity distributions of coherent and partially coherent higher-order ChG beams propagating through non-Kolmogorov turbulence are depicted in Fig. 1. It is necessary to note that the non-Kolmogorov spectrum parameters are set as $\alpha=3.8$, $L_0=1$ m, $l_0=0.01$ m and $\tilde{C}_n^2=1\times10^{-14}$ m$^{3-\alpha}$, and the other beam parameters are adopted as $n=3$, $\lambda=0.85$ μm, $w_0=0.02$ m and $\Omega_0=60$ m^{-1}. From Fig. 1 we can see that, with increase in propagation distance through non-Kolmogorov turbulence, the central dip of the hollow shape gradually disappears, the dark hollow beam tends to a flattened distribution and finally evolves into a Gaussian-like profile, which agrees well with the results reported in [8,9,26]. Moreover, under the same conditions, the central dip of the fully coherent higher-order ChG beam or the beam with higher spatial coherence can be sustained for longer propagation distance. This may be caused by the fact that the fluctuation of the source field increases as the coherence decreases. Figs. 2–4 show the normalized average intensity distribution, the rms beam width and the normalized M^2-factor of partially coherent higher-order ChG beams for different values of beam order, decentered parameter and initial coherence on

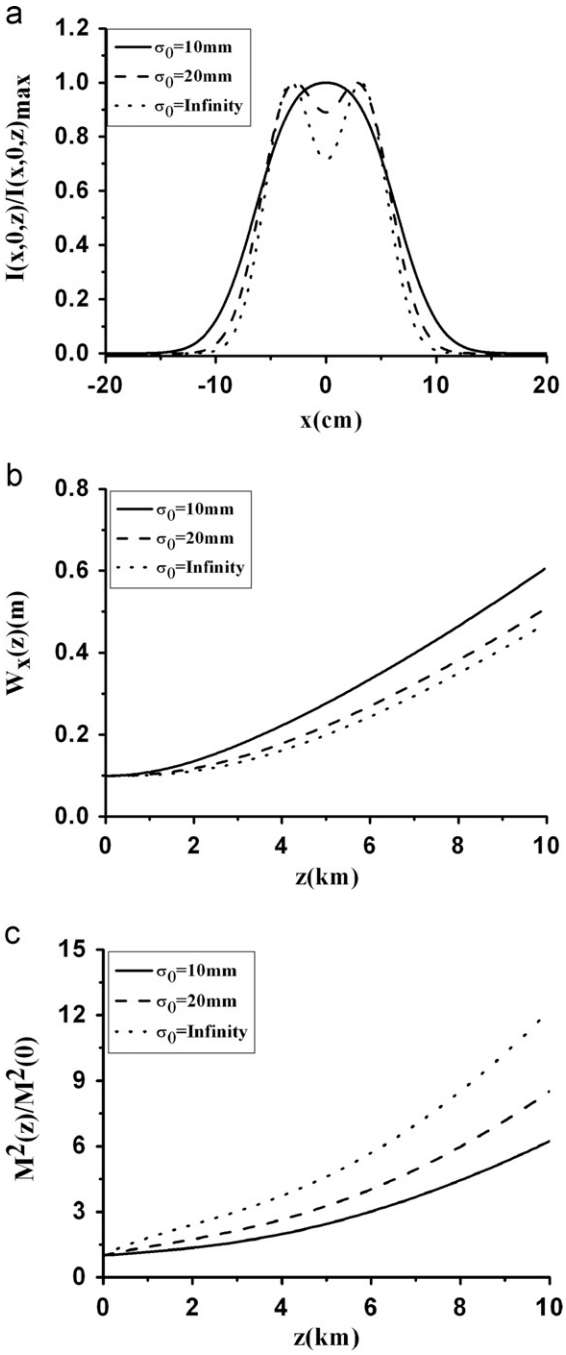

Fig. 4. Normalized average intensity distribution at $z=2$ km, the rms beam width and the normalized M^2-factor of partially coherent higher-order ChG beams for different values of the initial coherence on propagation in non-Kolmogorov turbulence. The other calculation parameters are $n=3$, $w_0=0.02$ m, and $\Omega_0=60$ m^{-1}.

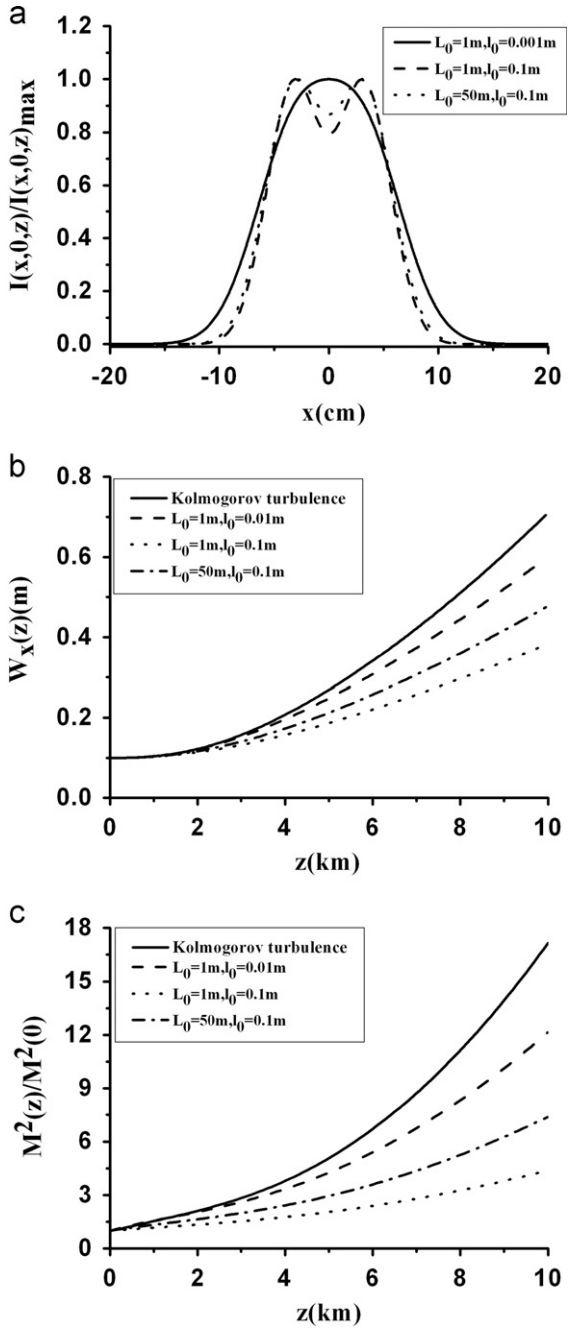

Fig. 5. Normalized average intensity distribution at $z=2$ km, the rms beam width and the normalized M^2-factor of partially coherent higher-order ChG beams on propagation both in Kolmogorov turbulence and in non-Kolmogorov turbulence for different outer scale and inner scale, respectively. The beam calculation parameters are $n=3$, $w_0=0.02$ m, $\Omega_0=60$ m^{-1} and $\sigma_0=0.02$ m, and the turbulence parameters are set as $\alpha=3.667$, and $\tilde{C}_n^2=1\times10^{-14}$ m$^{3-\alpha}$ for non-Kolmogorov turbulence, and $C_n^2=1\times10^{-14}$ m$^{-2/3}$ for Kolmogorov turbulence.

propagation in non-Kolmogorov turbulence, respectively. For the case of beam order $n=1$, the partially coherent higher order ChG beam reduces to the partially coherent ChG beam. As can be expected by Ref. [26], the conversion of the average intensity distribution of partially coherent higher-order ChG beams with smaller beam order or decentered parameter is quicker than that with larger one. One finds from Figs. 2 and 3(b) that the partially coherent higher-order ChG beam with the large beam order or decentered parameter has the large effective beam size in the source plane; however, the beam with smaller beam parameters spreads more rapidly with increasing the propagation distance, and the apparent distinction will disappear after propagating over a sufficiently long distance. As shown in Fig. 4 (a) and (b), the behavior of the normalized average intensity distribution and the rms beam width are also closely determined by the initial coherence of the beam. As seen from Figs. 2–4(c), the normalized M^2-factor increase more rapidly with smaller beam order, smaller decentered parameter or larger initial coherence. One comes to the conclusion that we can use partially coherent higher order ChG beams instead of ChG beams to improve system performance in turbulence atmosphere.

Figs. 5–7 show the normalized average intensity distribution, the rms beam width and the normalized M^2-factor of partially

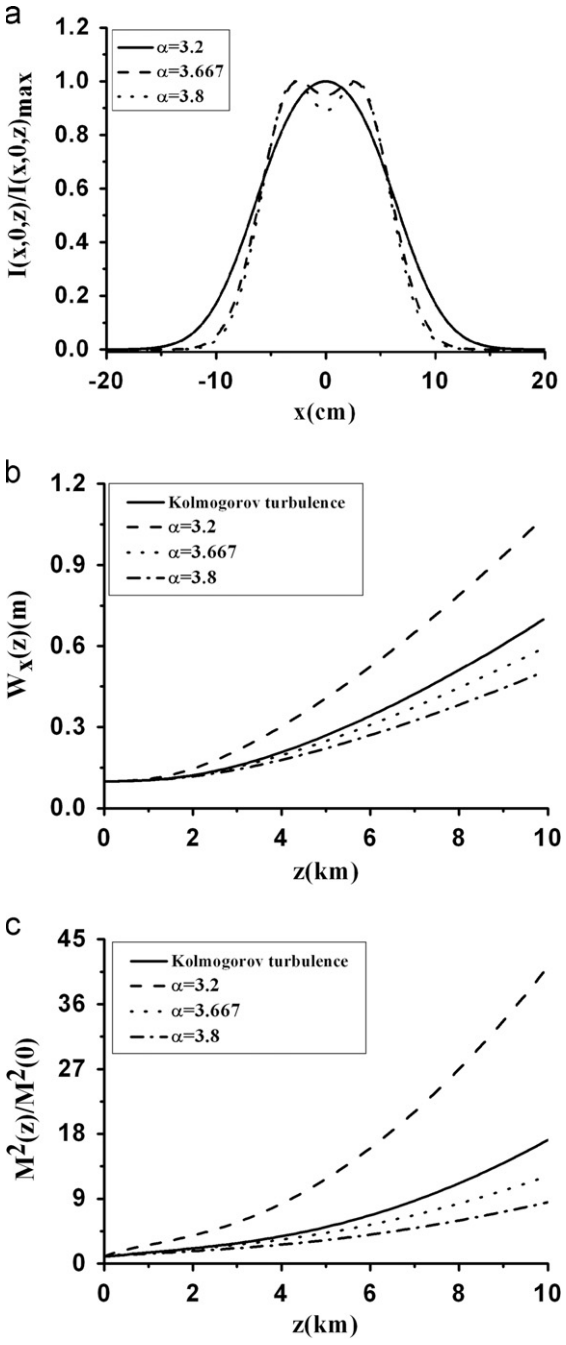

Fig. 6. Normalized average intensity distribution at $z=2$ km, the rms beam width and the normalized M^2-factor of partially coherent higher-order ChG beams in Kolmogorov turbulence and in non-Kolmogorov turbulence for different parameter α, respectively. The beam calculation parameters are the same as Fig.5, the turbulence parameters are set as $L_0=1$ m, $l_0=0.01$ m, and $\tilde{C}_n^2=1\times10^{-14}$ m$^{3-\alpha}$ for non-Kolmogorov turbulence, and $C_n^2=1\times10^{-14}$ m$^{-2/3}$ for Kolmogorov turbulence.

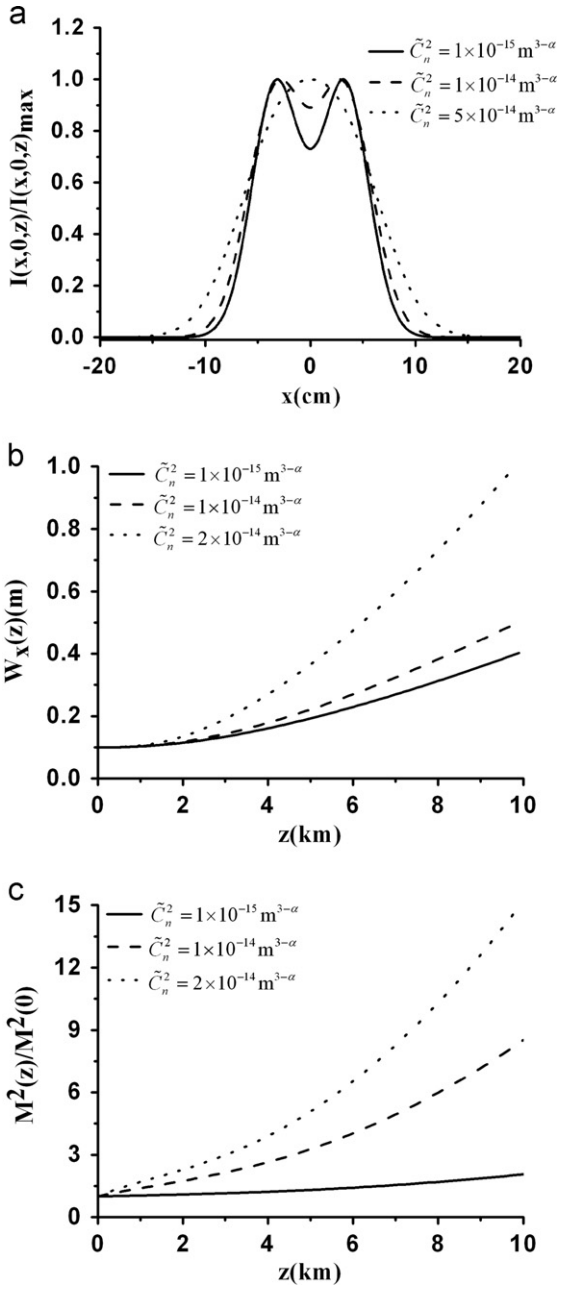

Fig. 7. Normalized average intensity distribution at $z=2$ km, the rms beam width and the normalized M^2-factor of partially coherent higher-order ChG beams for different values of the decentered parameter on propagation in non-Kolmogorov turbulence. The other calculation parameters are $n=3$, $w_0=0.02$ m, $\Omega_0=60$ m^{-1},$\sigma_0=0.02$ m, $\alpha=3.8$, $L_0=1$ m, and $l_0=0.01$ m.

coherent higher-order ChG beams on propagation in turbulent atmosphere for different outer scale, inner scale, parameter α and structure constant, respectively. From Figs. 5–7(a) it is seen that the hollow shape evolves into a Gaussian profile more rapidly in the turbulence with smaller inner scale, larger outer scale, smaller parameter α or larger structure constant. In Fig. 5(b) and (c), in order to compare the results in non-Kolmogorov turbulence with that in Kolmogorov turbulence, the turbulence condition is set to be $\alpha=3.667$ and $\tilde{C}_n^2=1\times10^{-14}$ m$^{3-\alpha}$ for non-Kolmogorov turbulence, and $C_n^2=1\times10^{-14}$ m$^{-2/3}$ for Kolmogorov turbulence. It is clear from Fig. 5(b) and (c) that the propagation properties of partially coherent higher-order ChG beams in non-Kolmogorov turbulence are much different from that in the case of conventional Kolmogorov turbulence. It is largely dependent on the outer scale and inner scale. The rms beam width and the normalized M^2-factor of the beams spread more rapidly with decreasing inner scale l_0 or increasing outer scale L_0 in non-Kolmogorov turbulence. It is seen from Fig. 6(b) and (c) that the propagation property of partially coherent higher-order ChG beams are also closely dependent on the exponent α in non-Kolmogorov turbulence. In addition, as indicated by Fig. 7, the rms beam width and the normalized M^2-factor of the beams spread more rapidly in the turbulence for a larger structure constant. The results can be interpreted physically as follows. The inner scale l_0 forms the lower limit of the inertial range and the outer scale L_0 forms the

upper limit of the inertial range. It is to be noted that decrease in inner-scale parameter and increase in outer-scale parameter corresponds to atmosphere turbulence with more intensity. The beam will be affected more in a stronger turbulence because of the larger wave front randomness. As a result, the partially coherent higher-order ChG beam will be more affected in non-Kolmogorov turbulence with smaller inner scale, larger outer scale or larger structure constant.

Fig. 8 shows the rms beam width of partially coherent higher-order ChG beams versus the propagation distance z in non-Kolmogorov turbulence with $\tilde{C}_n^2 = 10^{-14}\ \mathrm{m}^{3-\alpha}$ and in free space for different values of initial coherence, other parameters are the same as Fig. 1. It is clear from Fig. 8 that when the initial coherence is very small, there is no distinct difference between the spreading properties of partially coherent higher-order ChG beams in turbulence and in free space. As the initial coherence increases, the difference becomes apparent, and the difference is quite evident for fully coherent beams. One comes to the conclusion that partially coherent higher-order ChG beams with smaller initial coherence length are less affected by the turbulence although the beams with smaller initial coherence have greater spreading both in turbulent atmosphere and in free space. The physical interpretation is that the beams with lower initial coherence will suffer larger wave front randomness on their propagation, and the existence of substantial original randomness on wave front reduces the effect of turbulent atmosphere. The results are in good agreement with previous results of [30,31].

To further learn about the influence of other parameters on the spreading properties of partially coherent higher-order ChG beams in non-Kolmogorov turbulence, numerical results are compiled in Fig. 9. The plot, shown in Fig. 9(a), illustrates the impact of α variation on the spreading performance of partially coherent higher-order ChG beams in non-Kolmogorov turbulence for different initial coherence width. As indicated by Fig. 9(a), there is a remarkable increase of the rms beam width with the increasing of α and consequently a major penalty on system performance. However, after it reaches its maximum value (approximately $\alpha = 3.078$), the curve changes its slope and gradually decreases because the term $A(\alpha)$ begins to decrease to zero. The obvious physical interpretation of α approaching 3 is that the turbulence power spectrum tends to vanish. On the other hand, in the limiting case of α being close to 4, the power spectrum contains fewer eddies of high wave numbers, i.e. the wave front tilt is the primary aberration, leading to an improvement on the beam spreading. It is indicated, in non-Kolmogorov turbulence, that the beam spreading is largely dependent on the generalized exponent α, which leads to the results much different from those in the case of Kolmogorov turbulence with $\alpha = 11/3$. Fig. 9(b) is a plot of the rms beam width of partially coherent higher-order ChG beams versus the initial Gaussian waist width w_0 for different values of the cosh-part parameter Ω_0. It is shown that the rms beam width decreases sharply with the increasing of w_0 when w_0 is extremely small; however, with further increases of w_0, the rms beam width gradually increases, and the beams with larger Ω_0 spread more quickly. The plot shown in Fig. 9(c) illustrates the impact of the cosh-part parameter Ω_0 variation on the beams spreading for different values of beam order, and the Gaussian width is set to $w_0 = 0.02$ m. Notice that, when the parameter Ω_0 is very small ($\Omega_0 \le 30\ \mathrm{m}^{-1}$), the rms beam width does not seem to

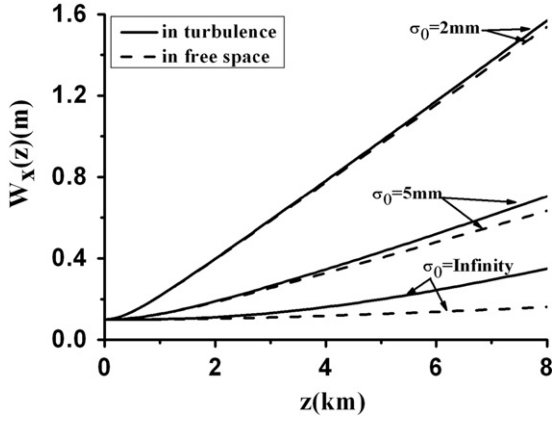

Fig. 8. The rms beam width of partially coherent higher-order ChG beams in non-Kolmogorov turbulence and in free space with different values of initial coherence. The other parameters are the same as Fig. 1.

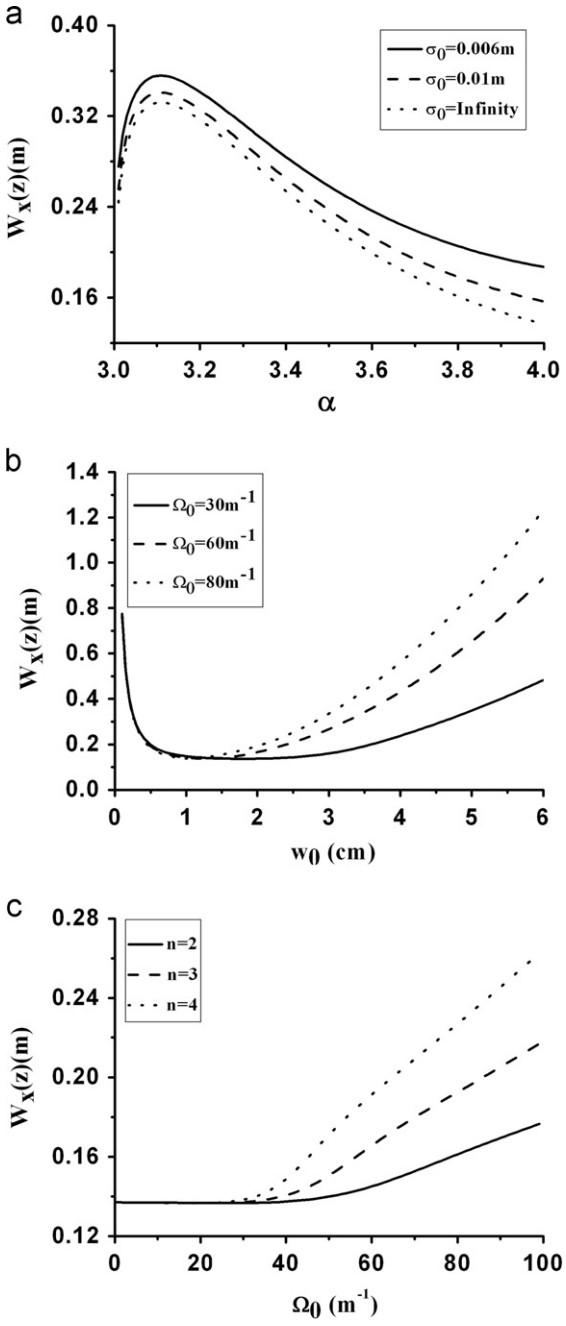

Fig. 9. The rms beam width of partially coherent higher-order ChG beams as a function of α, σ_0, w_0 and Ω_0 in the reference plane of $z = 2$ km in non-Kolmogorov turbulence.

change appreciably with Ω_0, and there is no distinct difference between the spreading properties of partially coherent higher-order ChG beams with different beam orders. The results can be physically interpreted as follows. For a small value of the parameter w_0 or Ω_0, the intensity profile of the partially coherent higher-order ChG beam is similar to a Gaussian distribution, and the corresponding effective beam width is equal to the Gaussian width w_0 in the source plane, so it almost shows the same spreading properties. The larger w_0, Ω_0 or n means the larger effective beam width. This is the physical reason why the rms beam width of partially coherent higher-order ChG beams increases with the further increase of w_0, Ω_0 and n.

4. Conclusions

In the present paper, the analytical formulas for the average intensity, the rms beam width and M^2-factor of partially coherent higher-order cosh-Gaussian beams in non-Kolmogorov turbulence have been derived by use of the extended Huygens–Fresnel principle and definition of the WDF. We mainly concentrate on the influences of different beam parameters and turbulence parameters on the propagation characteristics of partially coherent higher-order ChG beams in non-Kolmogorov turbulence. It has been found that partially coherent higher-order ChG beams with higher beam order, larger decentered parameter and smaller coherence length are less affected by the turbulence. It means that one may use partially coherent higher-order ChG beams as special cases of ChG beams to improve the system performance on propagation in turbulent atmosphere. The decreasing inner scale l_0, or increasing outer scale L_0 or the structure constant is equivalent to the increasing strength of the turbulence, and as a result, the partially coherent higher-order ChG beam will be more affected. Results show that the inner and outer scale, the exponent value α and the structure constant have serious influences on the beam propagation properties through non-Kolmogorov turbulence and is different from that in the case of Kolmogorov turbulence; that is, $\alpha=11/3$. It is to be noted that our results will be useful for the practical applications of the partially coherent higher-order ChG beams, such as remote sensing and optical communications.

Acknowledgements

Jun Qu acknowledges the support by the AnHui Provincial Natural Science Foundation of China under Grant no.11040606M154. Wei Huang acknowledges the support by the National Natural Science Foundation of China under Grant no. 21033008.

References

[1] Belenkii MS, Barchers JD, Karis SJ, Osmon CL, Brown JM, Fugate RQ. Preliminary experimental evidence of anisotropy of turbulence and the effect of non-Kolmogorov turbulence on wave front tilt statistics. Proceedings of SPIE 1999;3762:396–406.
[2] Gurvich A, Belen′kii M. Influence of stratospheric turbulence on infrared imaging. Journal of the Optical Society of America A 1995;12:2517–22.
[3] Toselli I, Andrews LC, Phillips RL, Ferrero V. Free-space optical system performance for laser beam propagation through non-Kolmogorov turbulence. Optical Engineering 2008;47:026003.
[4] Shchepakina E, Korotkova O. Second-order statistics of stochastic electromagnetic beams propagating through non-Kolmogorov turbulence. Optics Express 2010;18:10650–8.
[5] Luo H, Xu H, Cui Z, Qu J. Beam propagation factor of partially coherent Laguerre–Gaussian beams in non-Kolmogorov turbulence. Progress In Electromagnetics Research M 2012;22:205–18.
[6] Chu X. Evolution of beam quality and shape of Hermite–Gaussian beam in non-kolmogorov turbulence. Progress In Electromagnetics Research 2011;120:339–53.
[7] Xu H, Cui Z, Qu J. Propagation of elegant Laguerre–Gaussian beam in non-Kolmogorov turbulence. Optics Express 2011;19:21163–73.
[8] Chu X, Qiao C, Feng X. The effect of non-Kolmogorov turbulence on the propagation of cosh-Gaussian beam. Optics Communications 2010;283:3398–403.
[9] Tao R, Si L, Ma Y, Zhou P, Liu Z. Relay propagation of partially coherent cosh-Gaussian beams in non-Kolmogorov turbulence. Progress In Electromagnetics Research 2012;131:495–515.
[10] Zhou P, Ma Y, Wang X, Zhao H, Liu Z. Average spreading of a Gaussian beam array in non-Kolmogorov turbulence. Optics Letters 2010;35:1043–5.
[11] Wu G, Guo H, Yu S, Luo B. Spreading and direction of Gaussian–Schell model beam through a non-Kolmogorov turbulence. Optics Letters 2010;35:715–7.
[12] Toselli I, Andrews LC, Phillips RL, Ferrero V. Angle of arrival fluctuations for free space laser beam propagation through non kolmogorov turbulence. Proceedings OF SPIE 2007;6551:65510E-1.
[13] Eyyuboğlu H. Scintillation behavior of cos, cosh and annular Gaussian beams in non-Kolmogorov turbulence. Applied Physics B 2012;108:335–43.
[14] Zhang Y, Song Y, Chen Z, Ji J, Shi Z. Virtual sources for a cosh-Gaussian beam. Optics Letters 2007;32:292–4.
[15] Chu X. Propagation of a cosh-Gaussian beam through an optical system in turbulent atmosphere. Optics Express 2007;15:17613–8.
[16] Eyyuboğlu H. Annular, cosh and cos Gaussian beams in strong turbulence. Applied Physics B 2011;103:763–9.
[17] Eyyuboğlu H, Baykal Y, Cai Y. Degree of polarization for partially coherent general beams in turbulent atmosphere. Applied Physics B 2007;89:91–7.
[18] Eyyuboğlu H, Baykal Y. Analysis of reciprocity of cos-Gaussian and cosh-Gaussian laser beams in a turbulent atmosphere. Optics Express 2004;12:4659–74.
[19] Zhou G. Generalized beam propagation factors of truncated partially coherent cosine-Gaussian and cosh-Gaussian beams. Optics and Laser Technology 2010;42:489–96.
[20] Chu X. Moment and kurtosis parameter of partially coherent cosh-Gaussian beam in turbulent atmosphere. Applied Physics B 2011;103:1013–9.
[21] Zhou G, Chu X. Propagation of a partially coherent cosine-Gaussian beam through an ABCD optical system in turbulent atmosphere. Optics Express 2009;17:10529–34.
[22] Yang A, Zhang E, Ji X, Lü B. Angular spread of partially coherent Hermite–cosh-Gaussian beams propagating through atmospheric turbulence. Optics Express 2008;16:8366–80.
[23] Chu X, Ni Y, Zhou G. Propagation of cosh-Gaussian beams diffracted by a circular aperture in turbulent atmosphere. Applied Physics B 2007;87:547–52.
[24] Du X, Zhou G. Propagation of elliptical cosh-Gaussian beams and off-axial elliptical cosh-Gaussian beams in apertured optical systems. Applied Physics B 2007;88:267–72.
[25] Zhou G, Zheng J. Beam propagation of a higher-order cosh-Gaussian beam. Optics and Laser Technology 2009;41:202–8.
[26] Zhou G. Propagation of a higher-order cosh-Gaussian beam in turbulent atmosphere. Optics Express 2011;19:3945–51.
[27] Zhu S, Cai Y, Korotkova O. Propagation factor of a stochastic electromagnetic Gaussian Schell-model beam. Optics Express 2010;18:12587–98.
[28] Dan Y, Zhang B. Beam propagation factor of partially coherent flat-topped beams in a turbulent atmosphere. Optics Express 2008;16:15563–75.
[29] Yuan Y, Cai Y, Qu J, Eyyuboglu H, Baykal Y. Propagation factors of Hermite–Gaussian beams in turbulent atmosphere. Optics and Laser Technology 2010;42:1344–8.
[30] Wang F, Cai Y, Eyyuboğlu H, Baykal Y, Çil C. Partially coherent elegant Hermite–Gaussian beams. Applied Physics B 2010;100:617–26.
[31] Wang F, Cai Y, Eyyuboğlu H, Baykal Y. Average intensity and spreading of partially coherent standard and Elegant Laguerre–Gaussian beam in turbulent atmosphere. Progress In Electromagnetics Research 2010;103:33–56.
[32] Zhong Y, Cui Z, Shi J, Qu J. Polarization properties of partially coherent electromagnetic elegant Laguerre–Gaussian beams in turbulent atmosphere. Applied Physics B 2011;102:937–44.